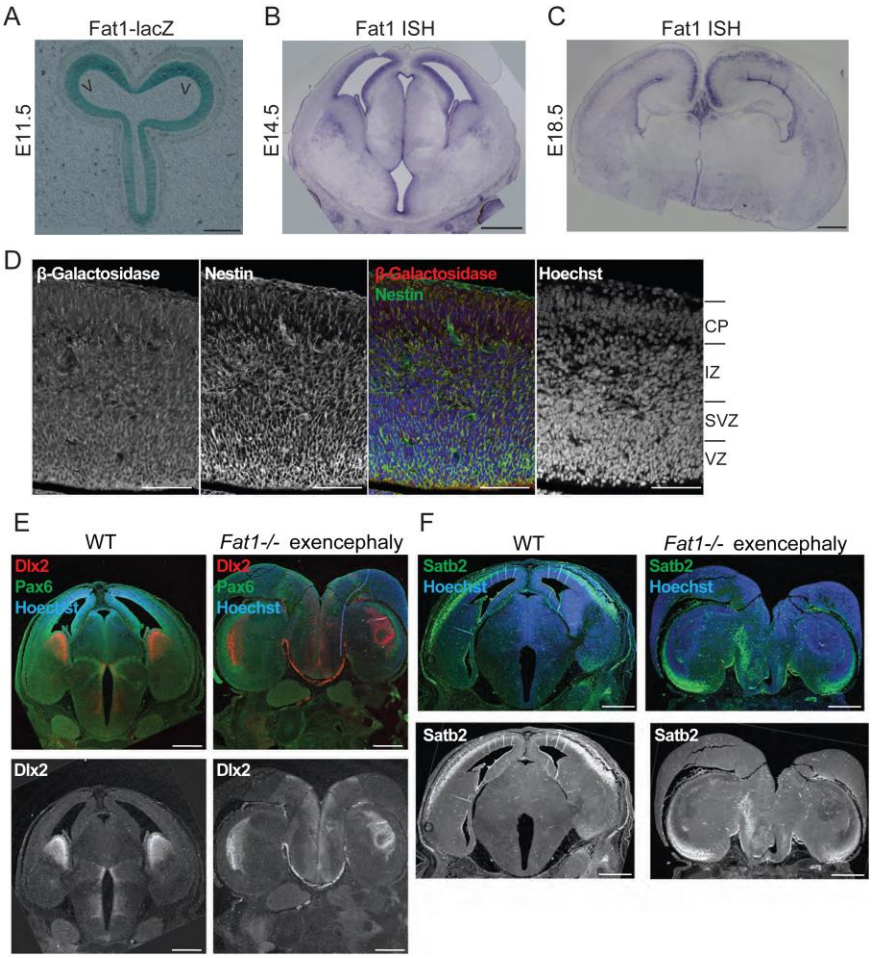

Figure S1. Fat1 is expressed in the developing brain

(A) Section through E11.5 *Fat1*$^{+/-}$ brain stained for β-Galactosidase to assess Fat1-lacZ expression. Scale bars, 100µm. (B,C) Fat1 expression in a coronal section from E14.5 (B) and E18.5 (C) brains revealed by in situ hybridization. Scale bar, 500µm. (D) Coronal section through E14.5 brain stained for β-Galactosidase (red) and the cortical precursor marker Nestin (green). Scale bars, 50µm. (E-F) Coronal section through E14.5 *Fat1*$^{-/-}$ exencephalic brain and control sibling stained for the ventral telencephalon marker Dlx2 (red) and the cortical precursor marker Pax6 (green) (E) and the neuronal marker Satb2 (green) (F) and Hoechst. Scale bars, 500µm. VZ, Ventricular Zone; SVZ, Sub-Ventricular Zone; IZ, Intermediate Zone; CP, Cortical plate.

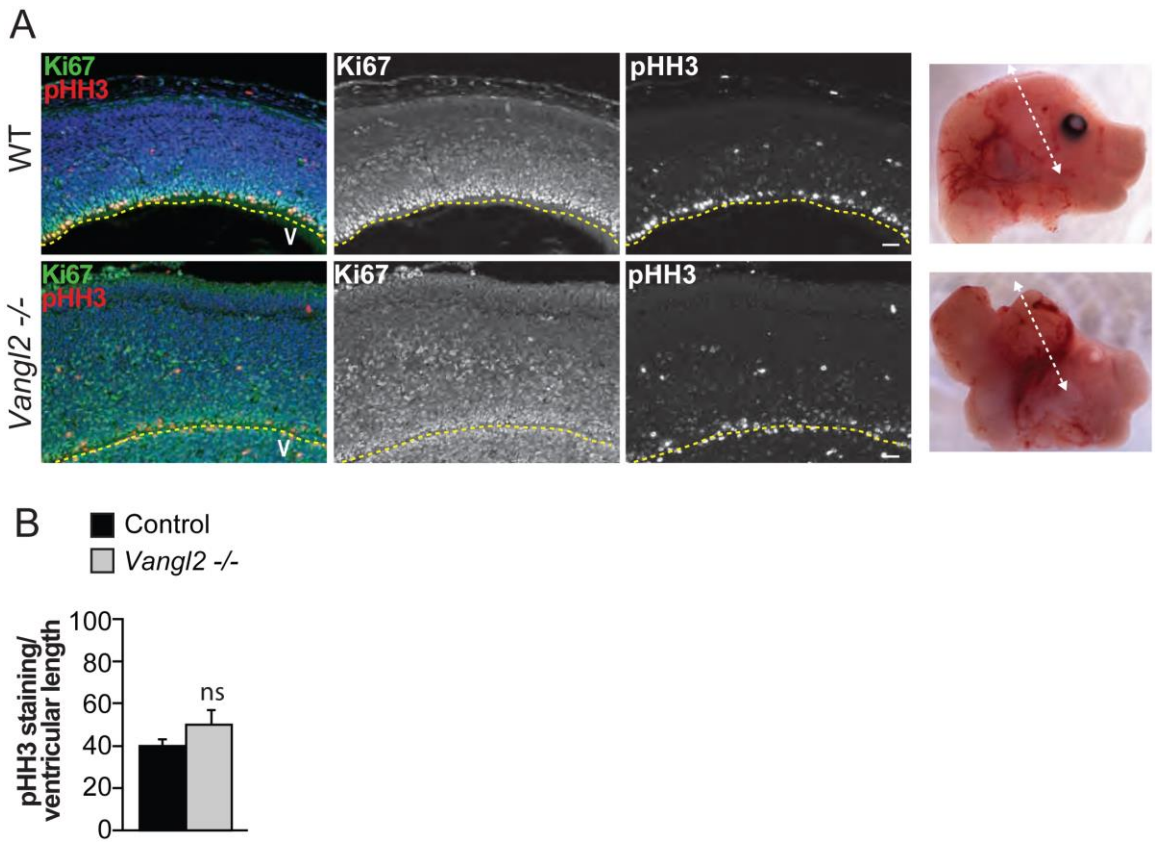

Figure S2. Proliferation of radial glial precursor is not increased in *Vangl2* mutants

(A) Confocal fluorescence micrographs from coronal sections of E14.5 *Vangl2*$^{-/-}$ embryos and a control sibling, stained for the proliferation marker Ki67 (green) and the mitotic marker pHH3 (red; left panel shows merge with hoechst). Corresponding embryos heads are on the right, with dashed arrows along the plane of sectioning. Capital V and yellow dashed line mark the ventricle. Scale bars, 20µm. (B) Quantification of the percentage of pHH3-positive cells calculated per ventricle length, in E14-15 *Vangl2*$^{-/-}$ embryonic cortices and control siblings. (n=5 controls and 4 *Vangl2* mutants, at least two different sections were measured for each).

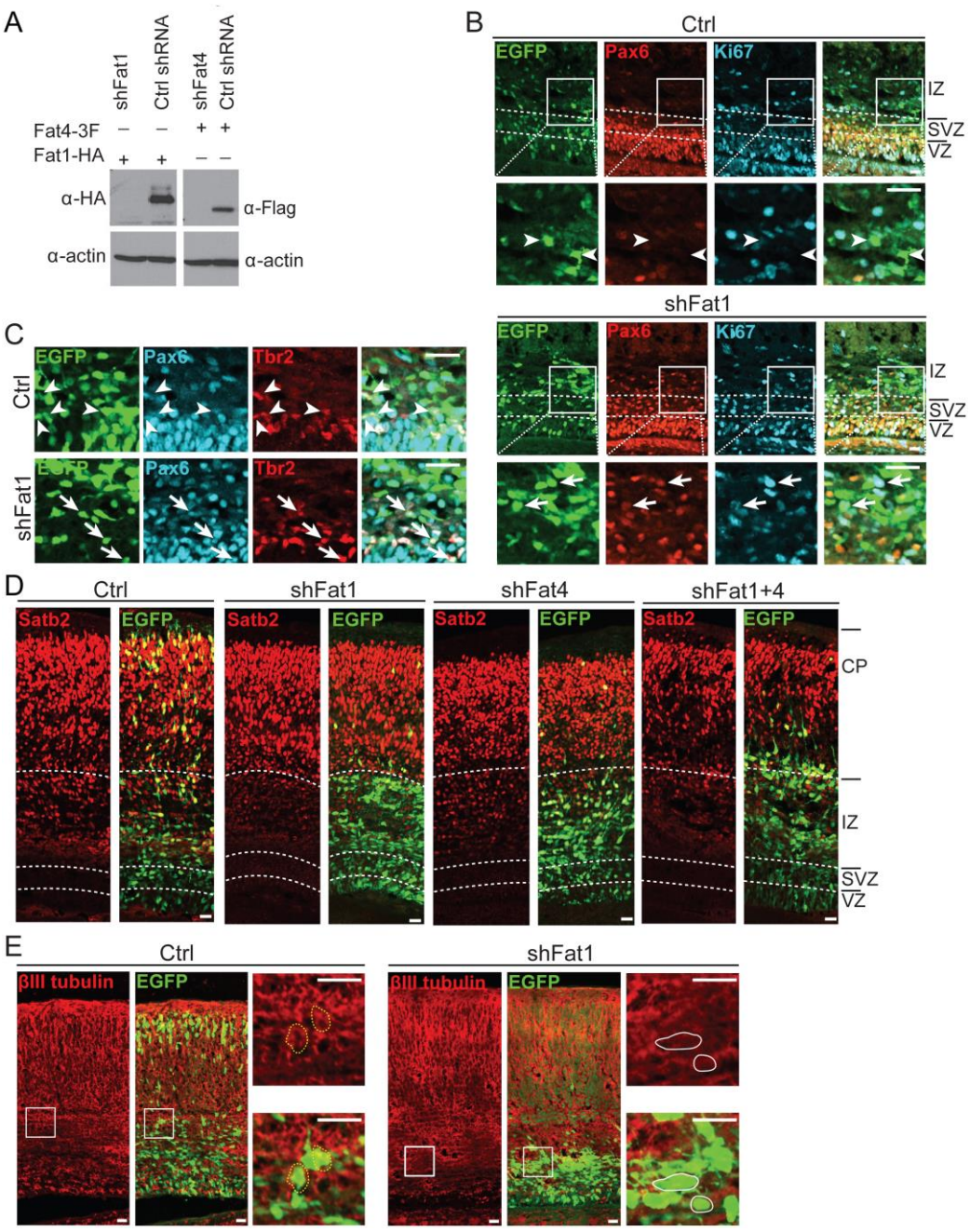

Figure S3.

(A) Western blot analysis of HEK 293 cell lysates after co-transfection with a Fat1-HA-tagged or a Fat4-Flag-tagged expression construct with Fat1 or Fat4 shRNAs. (B-E) E13/14 murine cortices electroporated with nuclear EGFP and a scrambled shRNA (Ctrl) or Fat1 shRNA (shFat1), and analyzed three days later at E16/17. (B) Confocal

fluorescence micrographs of coronal cortical sections immunostained for EGFP (green), Pax6 (red), and Ki67 (blue; right panel shows merge) . White lines demarcate different cortical regions, white boxes demarcate high magnification micrographs below. Arrows denote triple-labelled cells and arrowheads EGFP-positive cells negative for Pax6 and Ki67. Scale bar, 20μm. (C) Confocal micrographs of coronal sections immunostained for EGFP (green), Pax6 (blue), and Tbr2 (red; right panel shows merge). Arrows denote triple-labelled cells and arrowheads EGFP+, Pax6+ cells that are Ki67-negative. Scale bar, 20μm. (D) Low magnification fluorescence micrographs of coronal cortical sections immunostained for EGFP (green) and Satb2 (red). White lines demarcated different cortical regions. Scale bar, 20μm. (E) Fluorescence low maginification micrographs showing coronal cortical sections stained with βIII tubulin (red) and EGFP (green). White boxes demarcate high magnification micrographs below. White hatched line encircling EGFP+, βIII tubulin+ cells, white solid line encircling EGFP+, βIII tubulin-negative cells. Scale bar, 20μm.

A

129/B6

Genotype		Total Embryos	Exencephalic Embryos	% exencephalic
Fat1	*Fat4*			
Fat1 -/-	*Fat4 -/-*	0	0	**N/O**
Fat1 -/-	***Fat4 +/-***	**7**	**4**	**57%**
Fat1 -/-	***Fat4 +/+***	**5**	**1**	**20%**
Fat1 +/- or +/+	*Fat4 -/-*	8	0	**0%**
Fat1 +/- or +/+	*Fat4 +/- or +/+*	30	0	**0%**

CD-1

Fat1 -/-	*Fat4 -/-*	**15**	**4**	**27%**
Fat1 -/-	***Fat4 +/-***	**32**	**6**	**19%**
Fat1 +/-	***Fat4 -/-***	**44**	**1**	**2%**
Fat1 -/-	***Fat4 +/+***	**17**	**4**	**24%**
Fat1 +/+	*Fat4 -/-*	9	0	**0%**
Fat1 +/- or +/+	*Fat4 +/- or +/+*	159	0	**0%**

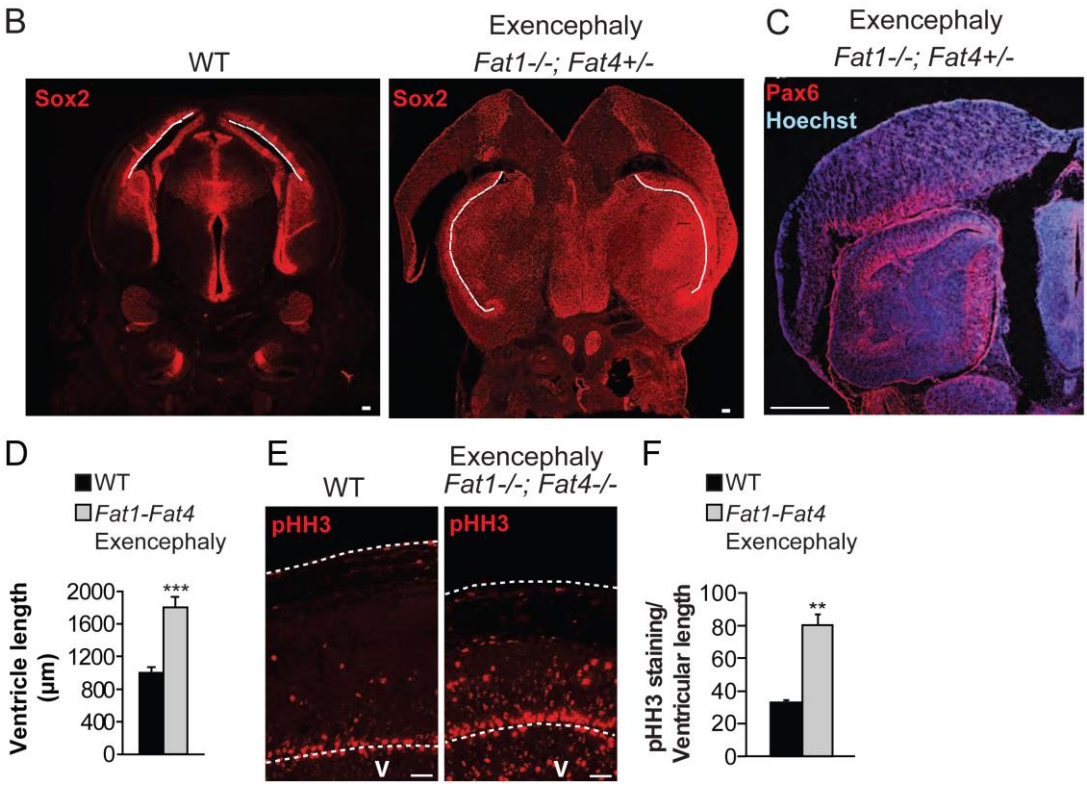

Figure S4. Loss of *Fat4* leads to an increase in the penetrance of *Fat1* exencephaly phenotype

(A) E13/15/16 embryos were obtained from *Fat1+/-; Fat4+/-* intercrosses in a mixed 129S6/SvEv - C57BL/6J (top) or in a CD-1 (bottom) genetic background. Numbers of progeny embryos with exencephaly are indicated for each genotype. N/O, non obtained

(B) Coronal sections from E15.5 *Fat1-/-; Fat4+/-* exencephalic brain and a control,

stained with Sox2. Dashed lines mark the lateral ventricles. (C) Coronal sections from E14.5 *Fat1-/-; Fat4+/-* exencephalic brain stained with Pax6. Sacle bar, 500µm (D) Quantification of posterior cortex length, from pictures similar to B and C (***p<0.001; n= 3 embryos each) (E) Coronal sections through E15.5 *Fat1-/-; Fat4+/-* exencephalic cortex and a control sibling stained for phospho-histone H3 (pHH3, red). Dashed lines indicate the apical (bottom) and basal (top) sides of the cortex. V, ventricle. (F) Quantification of the percentage of pHH3-positive cells calculated per ventricle length, from pictures as in E. Scale bars, 20µm (**p<0.01; n= 3 embryos each). Data are represented as mean ± SEM.

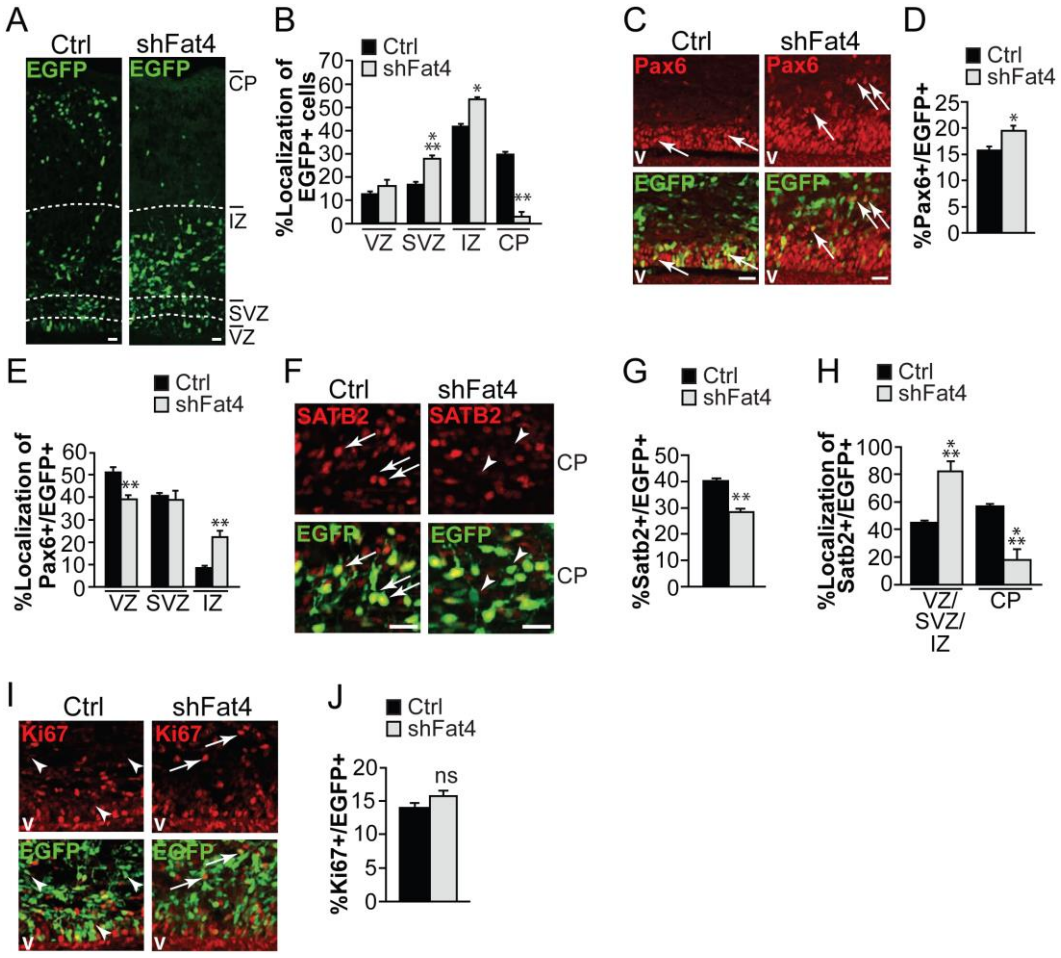

Figure S5. Fat4 knockdown promotes radial glial precursor proliferation

(A-J) Murine cortices were electroporated at E13.5 with a nuclear EGFP expression plasmid and Fat4 shRNA (shFat4) or a scrambled shRNA (Ctrl) plasmids, and analyzed three days later at E16/17. (A) Fluorescence confocal micrographs of E16.5 cortex stained for EGFP (green). Hatched white lines demarcate different cortical regions. (B) Quantification of sections as in A for the relative localization of EGFP positive cells. (*p<0.05; ***p<0.001; n=3 embryos each). (C) Confocal fluorescence micrographs from coronal sections through E16.5 cortex immunostained for Pax6 (red) and EGFP (green; lower panels show merge). (D,E) Quantification of sections as in (*C*) for the percentage

of Pax6+, EGFP+ cells per section (D) (*p<0.05), and relative localization in the VZ. SVZ, or IZ (E)(**p<0.01; n=3 embryos each). (F) Fluorescence confocal micrographs of the CP from coronal E16.5 cortical sections stained for Satb2 (red) and EGFP (green; right panel shows merge). (G,H) Quantification of sections as in (*F, S3D*) for the proportion of Satb2+, EGFP+ cells per section (G)(**p<0.01; n=3 embryos each), and relative localization in the VZ/SVZ/IZ versus the CP (H)(***p<0.001). (I) Fluorescence confocal micrographs of VZ/SVZ/IZ from coronal E16.5 cortical sections immunostained for Ki67 (red) and EGFP (green; lower panel shows merge). (J) Quantification of sections as in I for the proportion of Ki67+, EGFP+ cells per section. (n=3 embryos each). Arrowheads denote EGFP+ cells negative for respective marker and arrows denote double labelled cells. Scale bars, 20μm. ventricle; VZ, Ventricular Zone; SVZ, Sub-Ventricular Zone; IZ, Intermediate Zone; CP, Cortical plate. Error bars denote S.E.M.

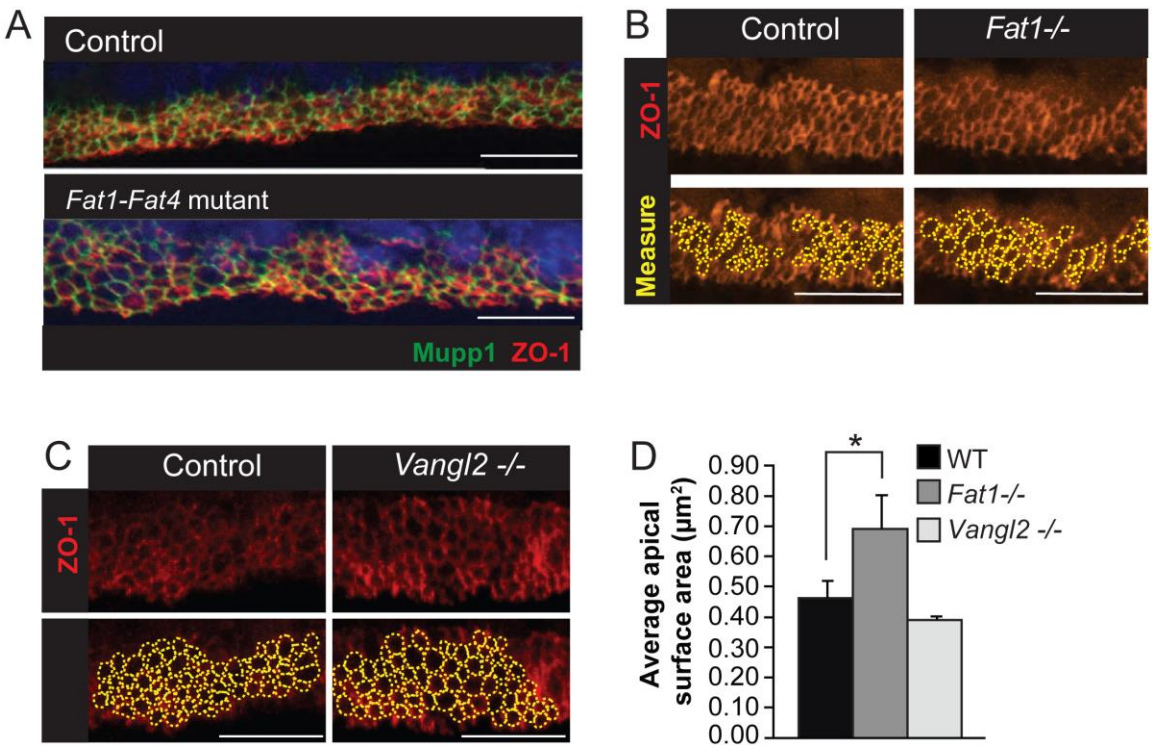

Figure S6. *Fat1* exencephalic mutants, but not *Vangl2*, have apical constriction defects

(A) Reconstruction of radial precursors apical surface in a *Fat1-/-; Fat4-/-* E14.5 cortex and a control sibling stained for ZO-1 (red) and Mupp1 (red). Scale bar, 5µm. (B,C) Radial glial progenitor apical domains 3D reconstructions from E14.5 *Fat1* exencephalic (B), *Vangl2* (C) mutants and controls, stained for ZO-1. Scale bar, 5µm. (C) Quantification of average apical surface area from images similar to those in B and C. (*$p<0.05$, n=10 control, n=4 *Fat1*$^{-/-}$ exencephalic embryos and n=4 *Vangl2*$^{-/-}$, at least 150 cells on 2 different sections were counted for each).

Protein	Top 4 control runs				FAT1-ICD run 1	FAT1-ICD run 2	FAT1-ICD SAINT	FAT4-ICD run 1	FAT4-ICD run 2	FAT4-ICD SAINT
KIF5B					920	875	**1.00**			
KLC2					695	667	**1.00**			
FAT1					**500**	**618**	**1.00**			
KIF5C					266	240	**1.00**			
KPNB1	26	20	5	2	205	180	**1.00**			
CSE1L					186	172	**1.00**			
PHB2					180	173	**1.00**			
PHB	4				113	108	**1.00**			
GCN1L1	5	4	2	2	73	44	**1.00**	14	4	
XPO1	1				69	61	**1.00**			
TNPO1					59	57	**1.00**			
ATAD3A	3				55	45	**1.00**	4		
RPN1	7				54	50	**1.00**		3	
PTPLAD1	13	4	4	2	51	46	**1.00**	12	13	
ATP5B	11	9	8	8	47	55	**1.00**	1		
C3orf39					47	37	**1.00**			
KLC1					44	46	**1.00**			
PEX19					31	23	**1.00**			
ATP5A1	9	8	6	5	29	28	**1.00**			
ATP2A2					27	31	**1.00**			
TNPO2					27	20	**1.00**			
ENAH					26	27	**1.00**			
IPO8					24	19	**1.00**			
KLC3					23	16	**1.00**			
HOMER1					21	19	**1.00**			
MTOR					20	9	**1.00**			
DCD	3	3	2	2	18	23	**1.00**			
SURF4					18	16	**1.00**			
VDAC2					17	13	**1.00**			
FIGF					17	12	**1.00**			
SEC61A1					14	13	**1.00**			
VDAC1					14	6	**1.00**			
XPOT					13	11	**1.00**			
STT3A					13	8	**1.00**	3		
FAT4								1176	1622	**1.00**
RPA1	10	3	2					165	154	**1.00**
LIX1L								107	97	**1.00**
DDX17	32	26	23	22	4	3		89	92	**1.00**
PARD3								85	81	**1.00**
RPS10-NUDT3	15	13	11	8	10	9		84	73	**1.00**
YBX1	31	19	18	17	21	23		82	90	**1.00**
C1QBP	10	9	6	6	9	7		82	84	**1.00**
TTC19								75	70	**1.00**
HSPD1	7	4	3	1	1			73	66	**1.00**
TIMM50	9	9	8	8	9	8		63	67	**1.00**
PMPCA								58	43	**1.00**
FRMPD1								57	42	**1.00**
USP9X								55	40	**1.00**
RPA3	7							45	35	**1.00**
PPP2R1A								45	34	**1.00**
SSBP1	6	4						43	45	**1.00**
BYSL	6	2						40	19	**1.00**
TRAF2								38	37	**1.00**
RPA2	2							34	24	**1.00**
FAM124A								34	21	**1.00**
PMPCB								31	34	**1.00**
PGAM5	3	3	1					31	31	**1.00**
MYL9								28	30	**1.00**
NOA1								23	46	**1.00**
PNMA2								23	19	**1.00**
CAD	3					2		23	13	**1.00**
CUL7								23	11	**1.00**
IGF2BP2								21	18	**1.00**
DNAJA3	4	2	2					18	18	**1.00**
MTDH	2							15	19	**1.00**
CDC20								15	16	**1.00**
C14orf169	1							14	12	**1.00**
AIM1								13	25	**1.00**
MOV10								13	7	**1.00**
MPP5								12	9	**1.00**
SND1								11	12	**1.00**
MPDZ								10	12	**1.00**
FBXW8								9	14	**1.00**
EMD	1							7	14	**1.00**
G3BP1	6	5	2					20	16	**0.99**
CALU	3					1		7	14	**0.98**
LARP1	5	3						12	14	**0.97**
EWSR1	7	7	6	5		1		27	18	**0.95**
IRS4	15	9	9	8				28	41	**0.94**
LUC7L3	7	7	3	3				18	14	**0.94**

Figure S7. Fat1 and Fat4 have different interactomes

MS data were analyzed as described in the text. Proteins identified with a SAINT score >0.9, and with >20 total peptides are shown. Known FAT1/4 binding partners are highlighted in blue. Proteins implicated in actin dynamics and junctions are highlighted in green. Bait proteins are highlighted in orange.

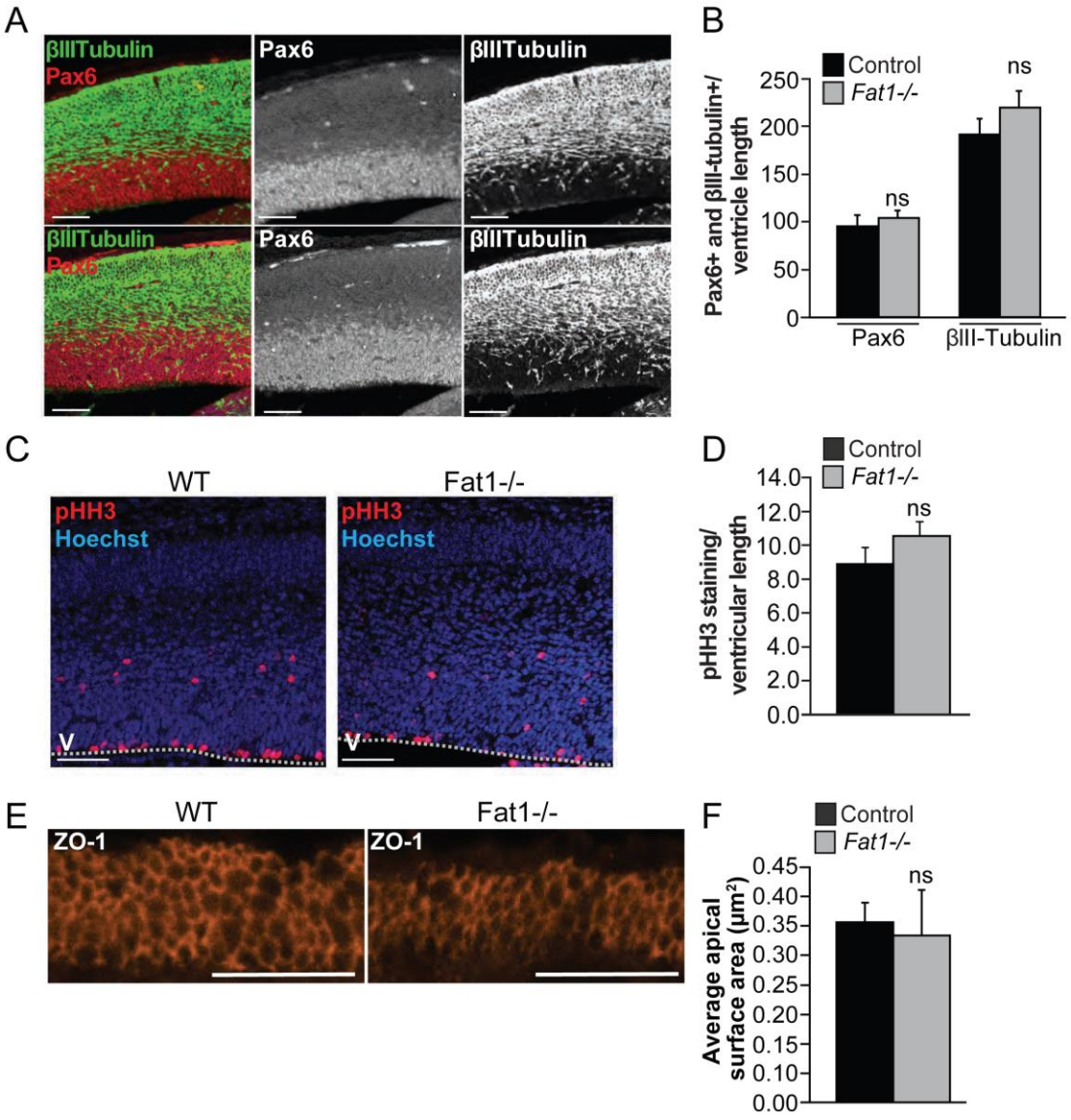

Figure S8. No increase in apical constriction or precursor proliferation in *Fat1* non exencephalic mutants

(A) Fluorescence confocal micrographs of *Fat1* non exencephalic mutant and control E14.5 cortex stained for Pax6 (red) and BIII-Tubulin (green). Scale bar, 100μm (B) Quantification of the percent Pax6+ and bIII-Tubulin+ areas in the dorsal cortex,

quantified from pictures as in A (n=3 embryos each). (C) Coronal sections through E14.5 *Fat1-/-* non exencephalic cortex and a control sibling stained for phospho-histone H3 (pHH3, red). Dashed lines indicate the basal side of the cortex. V, ventricle. Scale bar, 50µm (D) Quantification of the percentage of pHH3-positive cells per section calculated per ventricle length, from pictures as in C (n=3 embryos each). (E) Radial glial progenitor apical domains 3D reconstructions from E14.5 *Fat1* non exencephalic and control sibling, stained for ZO-1. Scale bar, 5µm. (F) Quantification of average apical surface area from images similar to those in C. (n=3 embryos each, at least 150 cells on 2 different sections were counted for each). Data are represented as mean ± SEM.

Supplementary Methods

Mouse lines

The *Fat4*$^{2E11\ \Delta flox}$ allele was described previously (Saburi et al., 2008). *Fat1lacZneo* mice were a gift from Dr. Charles ffrench-Constant (University of Edinburgh, UK). *Vangl2*^{Lp} (*Vangl2*^{S464N}) mice were generously provided by Dr Phillipe Gros (McGill University, Canada). Mice were maintained by backcrossing to 129S6/SvEv, CD-1 or C57BL/6J inbred mice (The Jackson Laboratory, USA).

Antibodies for immunostaining

The following primary antibodies were used in this study: rabbit anti-GFP (1:5000; Abcam #ab290), chicken anti-GFP (1:1000; Abcam #ab13970), rabbit anti-Pax6 (1:1000; Covance #PRB-278P), rabbit anti-Tbr2 (1:250; Abcam #ab23345), mouse anti-Satb2 (1:400; Abcam #ab51502), mouse anti-Ki67 (1:200; BD Biosciences #550609), rabbit anti-Sox2 (1:200, Cell Signaling #3728S), rabbit anti-pHH3 (1:500; Millipore #MABE13), mouse anti-Zo-1 (1:500; Invitrogen #339100), rabbit anti-βGalactosidase (1:200; Invitrogen #A11132), mouse anti-Nestin (1:400; BD Bioscience #554002) and rabbit anti-Par3 (1:200, Millipore #07-330). Relevant Cy3- or FITC-conjugated secondary antibodies (Jackson Laboratories) were used for primary antibody detection.

ß-galactosidase (lacZ) staining of embryonic brains and sectioning

A protocol similar to Nagy et al. 2007 was followed with minor modifications (Nagy et al., 2007). Briefly, E14.5 brains were dissected out of the developing skull in cold PBS.

Embryonic brains were then fixed with 0.2% glutaraldehyde for 30min at room temperature. Subsequently, tissues were washed and permeabilized using a wash solution containing sodium deoxycholate (0.01%) and NP-40 (0.02%) with a pH of 8.4. Embryos were stained with an X-gal solution overnight at 4°C followed by a final overnight fixation with 4% PFA. For tissue embedding, brains were serially dehydrated and incubated in liquid paraffin overnight. Coronal sections of 10uM were carried out on a Leica microtome. The paraffin was cleared with Histo-Clear, rehydrated and counterstained with Fast Red. Sections were mounted and visualized on a bright-field microscope.

Plasmids

The nuclear EGFP expression plasmid was driven from the *EF1 α* promoter (pEF-EGFP), while the cytoplasmic EGFP expression plasmid was driven from the CAG promoter (pCAGGS-EGFP) as has been previously described (Wang et al., 2012). Fat1, Fat4 and scrambled negative control shRNAs were purchased from EZBiolabs (Carmel, IN) and expression of the targeted sequences was driven from the H1 promoter. The targeted sequences are 5'-GCAGAGGTTCAACCTGAATCA-3' for shFat1 and 5'-GCACAGATCCCTCTAGAATCT-3' for shFat4. The shRNA negative control target sequence is 5'-GTTCTCCGAACGTGTCACGT-3'.

Validation of Fat1 and Fat4 shRNA in HEK293 cells

HEK293 cells were grown to confluency and cotransfected with mouse Fat1 or Fat4 constructs lacking most of their extra-cellular domains, Fat1ΔECD and Fat4ΔECD. Cells

were co-transfected with Fat1, Fat4 or control shRNAs using Lipofectamine 2000 (Invitrogen). shRNA targeting the C-terminal part of Fat1 and Fat4 cDNA were generated by EzBiolab.

Cell culture, co-immunoprecipitation and western blotting

For Fat4 and Mupp1 co-immunoprecipitation: Flp-In™ 293 T-Rex™ stable inducible cell lines expressing either FLAG-tagged Fat4 intracellular domain or GFP were cultured in DMEM mammalian media (Life Technologies) containing 10% fetal bovine serum (Sigma), 1% penicillin-streptomycin, 100ug/ml Hygromycin B (Bioshop) and 1% GlutaMAX media supplement (Life Technologies). Cells were induced with tetracycline (0.5 ug/ml for GFP, 1 ug/ml for Fat4) and harvested 48 hours after induction.

For Fat4 and Fat1 co-immunoprecipitation: HEK293T cells were transfected, using calcium phosphate transfection, with pCMV5 plasmids encoding Fat1ΔECD-HA, Fat4ΔECD-Flag, Fat4-ICD-Flag and BMPRII-Flag as indicated, 48 hours before lysis. Cells were lysed in buffer (50 mM HEPES [pH 8.0], 100 mM KCL, 2 mM EDTA, 0.1% NP40, 1.0 mM PMSF, 10% glycerol, and protease cocktail inhibitor [Roche]). FLAG-immunoprecipitation was performed by using α-FLAG M2 agarose beads (Sigma). SDS sample buffer was added after five washes of the beads with the lysis buffer. Western blots were performed according to standard protocols. Antibodies used were mouse α-FLAG (1:10000, Sigma #F1804), mouse α-MUPP1 (1:1000, BD Biosciences #611558), Rat α-HA (1:6000, Roche #11867431001) and mouse α-Mena (1:1000, gift from Gertler lab).

Affinity purification

For MS analysis of interacting proteins, 6 × 150 cm^2 dishes of sub-confluent (80%) HEK 293 cells expressing the protein of interest were scraped into PBS, pooled, washed twice in 25 ml PBS, and collected by centrifugation at 1000 × *g* for 5 min at 4°C. Cell pellets were stored at -80°C until lysis. The cell pellet was weighed, and 1:4 pellet weight:lysis buffer (by volume) was added. Lysis buffer consisted of 50 mM HEPES-NaOH (pH 8.0), 100 mM KCl, 2 mM EDTA, 0.1% NP40, 10% glycerol, 1 mM PMSF, 1 mM DTT and 1:500 protease inhibitor cocktail (Sigma-Aldrich, St. Louis, MO). On resuspension, cells were incubated on ice for 10 min, subjected to one additional freeze–thaw cycle, then centrifuged at 27000 × *g* for 20 min at 4°C. Supernatant was transferred to a fresh 15 ml conical tube, and 1:1000 benzonase nuclease (Novagen) plus 30 ul packed, pre-equilibrated Flag-M2 agarose beads (Sigma-Aldrich) were added. The mixture was incubated for 2 h at 4°C with end-over-end rotation. Beads were pelleted by centrifugation at 1000 × *g* for 1 min and transferred with 1 ml of lysis buffer to a fresh centrifuge tube. Beads were washed once with 1 ml lysis buffer and twice with 1 ml ammonium bicarbonate (ammbic) rinsing buffer (50 mM ammbic, pH 8.0, 75 mM KCl). Elution was performed by incubating the beads with 150 ul of 125 mM ammonium hydroxide (pH >11). The elution step was repeated twice, and the combined eluate centrifuged at 15000 × *g* for 1 min, transferred to a fresh centrifuge tube and lyophilized.

Mass spectrometry

One microgram of MS-grade TPCK trypsin (Promega, Madison, WI) dissolved in 70 ul of 50 mM ammbic (pH 8.3) was added to the Flag eluate and incubated at 37°C

overnight. The sample was lyophilized and brought up in 0.1% formic acid. LC analytical columns (75 um inner diameter) and pre-columns (100 um inner diameter) were made in-house from fused silica capillary tubing from InnovaQuartz (Phoenix, AZ) and packed with 100 Å C_{18}-coated silica particles (Magic, Michrom Bioresources, Auburn, CA). Peptides were subjected to nanoflow liquid chromatography - electrospray ionization - tandem mass spectrometry (nLC-ESI-MS/MS), using a 90 min reversed phase (10-40% acetonitrile, 0.1% formic acid) buffer gradient running at 250 nL/min on a Proxeon EASY-nLC pump in-line with a hybrid linear quadrupole ion trap (Velos LTQ) Orbitrap mass spectrometer (Thermo Fisher Scientific, Waltham, MA). A parent ion scan was performed in the Orbitrap, using a resolving power of 60,000. Simultaneously, up to the tweny most intense peaks were selected for MS/MS (minimum ion count of 1000 for activation) using standard CID fragmentation. Fragment ions were detected in the LTQ. Dynamic exclusion was activated such that MS/MS of the same *m*/*z* (within a 10 ppm window, exclusion list size 500) detected three times within 45 sec were excluded from analysis for 30 sec.

For protein identification, Thermo .RAW files were converted to the .mzXML format using Proteowizard (Kessner et al., 2008), then searched against Human RefSeq Version 45 (containing 36113 entries, appended with a reversed decoy database of equal size based on RefSeq v45) using the Comet (Eng et al., 2013) search engine. Search parameters specified a parent MS tolerance of 15 ppm and an MS/MS fragment ion tolerance of 0.4 Da, with up to two missed cleavages allowed for trypsin. Oxidation of methionine was allowed as a variable modification. Each AP was analyzed using at least two technical replicates. Statistical validation of peptide and protein identifications was

performed using the Trans-Proteomic Pipeline (Keller and Shteynberg, 2011). For each search, the Protein Prophet probability at 1% error rate was used as a cutoff value to generate a matrix input file to upload to the CRAPome (v1.1). 12 in-house control runs (consisting of Flag alone, Flag-GFP, and unrelated Flag-tagged proteins) and 30 additional control datasets were selected from within the CRAPome (all FLAG-AP/MS data in HEK 293 cells). SAINTexpress options were; LowMode = 0, MinFold = 0, Normalize = 1, Virtual controls = 4, Controls = All Controls.

BrdU incorporation

BrdU solution containing 5-Bromo-2′ -deoxyuridine (10 mg/ml) was injected intraperitoneally in pregnant mice (50 mg BrdU/kg of mice) 24 hours before embryonic dissection. The samples were prepared and sectioned as described above before being incubated overnight with anti-mouse BrdU antibody (Clone Bu20a, Dako).

Eng, J. K., Jahan, T. A. and Hoopmann, M. R. (2013) 'Comet: an open-source MS/MS sequence database search tool', *Proteomics* **13**(1): 22-4.
Keller, A. and Shteynberg, D. (2011) 'Software pipeline and data analysis for MS/MS proteomics: the trans-proteomic pipeline', *Methods Mol Biol* **694**: 169-89.
Kessner, D., Chambers, M., Burke, R., Agus, D. and Mallick, P. (2008) 'ProteoWizard: open source software for rapid proteomics tools development', *Bioinformatics* **24**(21): 2534-6.
Saburi, S., Hester, I., Fischer, E., Pontoglio, M., Eremina, V., Gessler, M., Quaggin, S. E., Harrison, R., Mount, R. and McNeill, H. (2008) 'Loss of Fat4 disrupts PCP signaling and oriented cell division and leads to cystic kidney disease', *Nature genetics* **40**(8): 1010-5.
Wang, J., Gallagher, D., DeVito, L. M., Cancino, G. I., Tsui, D., He, L., Keller, G. M., Frankland, P. W., Kaplan, D. R. and Miller, F. D. (2012) 'Metformin activates an atypical PKC-CBP pathway to promote neurogenesis and enhance spatial memory formation', *Cell stem cell* **11**(1): 23-35.